SKB TECHNICAL REPORT 97-27

Temperature field due to time-dependent heat sources in a large rectangular grid

Application for the KBS-3 repository

Thomas Probert, Johan Claesson

Depts. of Mathematical Physics and Building Physics,
Lund University, Sweden

April 1997

SVENSK KÄRNBRÄNSLEHANTERING AB
SWEDISH NUCLEAR FUEL AND WASTE MANAGEMENT CO

P.O.BOX 5864 S-102 40 STOCKHOLM SWEDEN
PHONE +46 8 459 84 00
FAX +46 8 661 57 19

TEMPERATURE FIELD DUE TO TIME-DEPENDENT HEAT SOURCES IN A LARGE RECTANGULAR GRID

APPLICATION FOR THE KBS-3 REPOSITORY

Thomas Probert, Johan Claesson

Depts. of Mathematical Physics and Building Physics, Lund University, Sweden

April 1997

Information on SKB technical reports from1977-1978 (TR 121), 1979 (TR 79-28), 1980 (TR 80-26), 1981 (TR 81-17), 1982 (TR 82-28), 1983 (TR 83-77), 1984 (TR 85-01), 1985 (TR 85-20), 1986 (TR 86-31), 1987 (TR 87-33), 1988 (TR 88-32), 1989 (TR 89-40), 1990 (TR 90-46), 1991 (TR 91-64), 1992 (TR 92-46), 1993 (TR 93-34), 1994 (TR 94-33), 1995 (TR 95-37) and 1996 (TR 96-25) is available through SKB.

TEMPERATURE FIELD DUE TO TIME-DEPENDENT HEAT SOURCES IN A LARGE RECTANGULAR GRID.

II. Application for the KBS-3 repository.

Thomas Probert

Johan Claesson

April 1997

Depts. of Mathematical Physics and Building Physics
Lund University, Sweden

Keywords: Temperature field from heat sources, rectangular grid, three-dimensional time-dependent analytical solution, superposition, nuclear waste repository in rock, results for KBS-3 data.

Abstract

In the KBS-3 concept canisters containing nuclear waste are deposited along parallel tunnels over a large rectangular area deep below the ground surface. The temperature field in rock due to such a rectangular grid of heat-releasing canisters is studied.

An analytical solution for this problem for any heat source has been presented in a preceding paper. The complete solution is summarized in this paper.

The solution is by superposition divided into two main parts. There is a global temperature field due to the large rectangular canister area, while a local field accounts for the remaining heat source problem.

In this sequel to the first report, the local solution is discussed in detail. The local solution consists of three parts corresponding to line heat sources along tunnels, point heat sources along a tunnel and a line heat source along a canister. Each part depends on two spacial variables only. These parts are illustrated in dimensionless form.

Inside the repository the local temperature field is periodic in the horizontal directions and has a short extent in the vertical direction. This allows us to look at the solution in a parallelepiped around a canister. The solution in the parallelepiped is valid for all canisters that are not too close to the repository edges.

The total temperature field is calculated for the KBS-3 case. The temperature field is calculated using a heat release that is valid for the first 10 000 years after deposition. The temperature field is shown in 23 figures in order to illustrate different aspects of the complex thermal process.

Sammanfattning

I KBS-3 konceptet deponeras kaplsar innehållande radioaktivt avfall längs parallella tunnlar över ett stort rektangulärt område på stort djup. Temperaturfältet i berg från ett sådant rektangulärt fält av värmeavgivande kapslar studeras.

En analytisk lösning till detta problem för en godtycklig värmekälla har presenterats i en föregående rapport. Den kompletta lösningen sammanfattas i denna rapport.

Lösningen uppdelas genom superposition i två huvuddelar. En global del avser värmeavgivning över en rektangulär area, medan ett lokalt fält tar hand om lösningen för det resterande värmekällsproblemet.

I denna fortsättning studeras den lokala lösningen i detalj. Den lokala lösningen består av tre delar. Dessa delar svarar mot linjekällor längs tunnlar, punktkällor längs en tunnel och en linjekälla längs en kapsel. Varje del är en funktion av enbart två rumsvariabler. Dessa delar illustreras på dimensionslös form.

Det lokala temperaturfältet inom kapselområdet är periodiskt i de horisontella riktningarna och har kort räckvidd i den vertikala riktningen. Detta tillåter att vi tittar på lösningen i en parallellepiped kring en kapsel. Lösningen i parallellepipeden gäller för varje kapsel som inte är för nära förvarets kanter.

Det totala temperaturfältet beräknas för data från KBS-3. Temperaturfältet beräknas för en värmeavgivning som gäller under de första 10 000 åren. Temperaturfältet visas i 23 figurer vilka illustrerar olika aspekter på den komplicerade temperaturprocessen.

Contents

1 Introduction

This report is a direct sequel to (Claesson J, Probert T, Jan. 1996), which should be read first. The problem and analyses are not repeated here.

Figure 1 shows the tunnels of the nuclear waste repository. The heat releasing canisters are placed along the tunnels. There is a rectangular region with the area $D \cdot D'$ around each canister. See Figure 1, right.

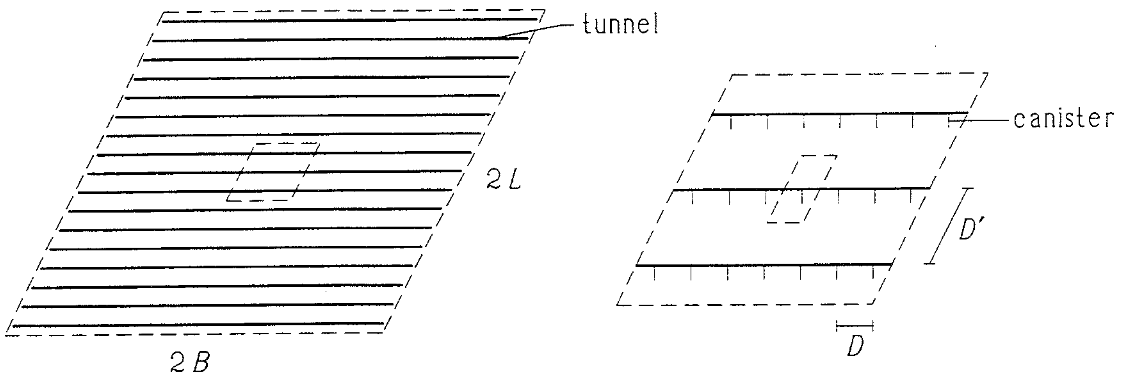

Figure 1: Tunnels and rectangular grid of canisters according to the SKB-3 concept. The right-hand figure shows an internal part with tunnels and canisters in greater detail.

The thermal problem is divided into a global and a local part. In the global part, there is a plane heat source $q_o(t) = Q_o(t)/(DD')$ (W/m^2) over the repository rectangle. See Figure 2. The remaining problem is discussed in Section 3. There, the plane heat source is subtracted as shown in Figure 3.

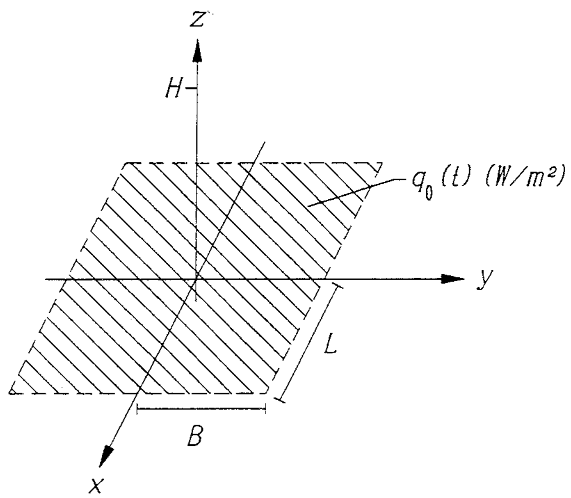

Figure 2: Plane heat source $q_o(t)$ (W/m^2) over the repository rectangle causing the global temperature.

The analytically determined total temperature field has been compared with a numerically determined temperature field with very good results. See (Hökmark H, 1996).

2 Global Solution

The global solution of the rectangular heat source is presented and illustrated in (Claesson J, Probert T, Jan. 1996). The temperature field from the rectangular heat source is obtained by superposition. It should be noted that the global temperature and all other temperatures in this study are the excess temperatures above undisturbed conditions. The global solution for any heat source $q_o(t)$ is given by:

$$T_{gl}(x,y,z,t) = \frac{1}{4\lambda}\sqrt{\frac{at_0}{\pi}} \cdot \int_0^{\sqrt{t/t_0}} q_0\left(t - t_0 s^2\right) \cdot \left[\operatorname{erf}\left(\frac{L-x}{s\sqrt{4at_0}}\right) + \operatorname{erf}\left(\frac{L+x}{s\sqrt{4at_0}}\right)\right] \cdot$$

$$\cdot \left[\operatorname{erf}\left(\frac{B-y}{s\sqrt{4at_0}}\right) + \operatorname{erf}\left(\frac{B+y}{s\sqrt{4at_0}}\right)\right] \cdot \left[e^{-z^2/(s^2 4at_0)} - e^{-(z-2H)^2/(s^2 4at_0)}\right] ds \quad (1)$$

The heat source may consist of a sum of exponentials:

$$q_0(t) = \sum_i q_i e^{-t/ti} \qquad q_i = \frac{Q_i}{DD'} \quad (2)$$

Then the global temperature is given by a sum of integrals. We have:

$$T_{gl}(x,y,z,t) = \sum_i T_{gl,i}(x,y,z,t) \quad (3)$$

The integrals $T_{gl,i}$ are given by:

$$T_{gl,i}(x,y,z,t) = \frac{q_i}{4\lambda} \cdot \sqrt{\frac{at_i}{\pi}} \int_0^{\sqrt{t/t_i}} e^{-t/t_i + s^2} \left[\operatorname{erf}\left(\frac{L-x}{s\sqrt{4at_i}}\right) + \operatorname{erf}\left(\frac{L+x}{s\sqrt{4at_i}}\right)\right] \cdot$$

$$\cdot \left[\operatorname{erf}\left(\frac{B-y}{s\sqrt{4at_1}}\right) + \operatorname{erf}\left(\frac{B+y}{s\sqrt{4at_i}}\right)\right] \cdot \left[e^{-z^2/(s^2 4at_i)} - e^{-(z-2H)^2/(s^2 4at_i)}\right] ds \quad (4)$$

These integrals must be evaluated numerically.

3 Local Solution

In the local solution the canisters are represented by point, line and plane heat sources (See Figure 3). The total heat release of a canister is $Q_0(t)$ (W). The canisters lie along the tunnels. The spacing between the canisters is D. In all tunnels in the repository except the central one, the canister heat sources are represented by line heat sources of strength $q_l(t)$:

$$q_l(t) = \frac{Q_0(t)}{D} \quad (\mathrm{W/m}) \quad (5)$$

The spacing between the tunnels is D'. The central tunnel along the y-axis is represented by a line of heat sources. All the canisters along this line except the central one are represented by point heat sources of strength $Q_0(t)$. The central canister is approximated by a finite line heat source of length H_c and strength $q_c(t)$:

$$q_c(t) = \frac{Q_0(t)}{H_c} \quad (\mathrm{W/m}) \quad (6)$$

All the heat sources are balanced by the plane heat source of strength $-q_0(t)$:

$$q_0(t) = \frac{Q_0(t)}{DD'} \quad (\mathrm{W/m^2}) \tag{7}$$

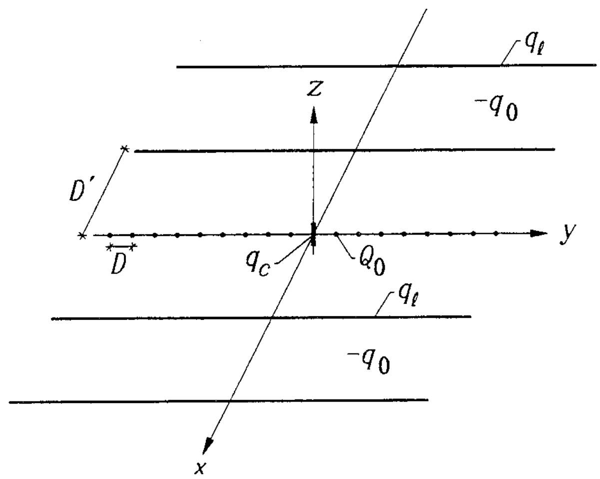

Figure 3: The heat sources of the local temperature field.

The local solution T_{loc} can be divided into three distinct parts corresponding to line heat sources along tunnels (index $l.s.$), point heat sources along a tunnel (index $p.s.$) and line heat source along the considered interior canister (index $l.c.$). We have:

$$T_{loc} = T_{l.s.} + T_{p.s.} + T_{l.c.} \tag{8}$$

All these heat sources are balanced. The first part $T_{l.s.}$ is the contribution from the line heat sources along the tunnels q_l balanced by a plane heat sink $-q_0$ (See Figure 4).

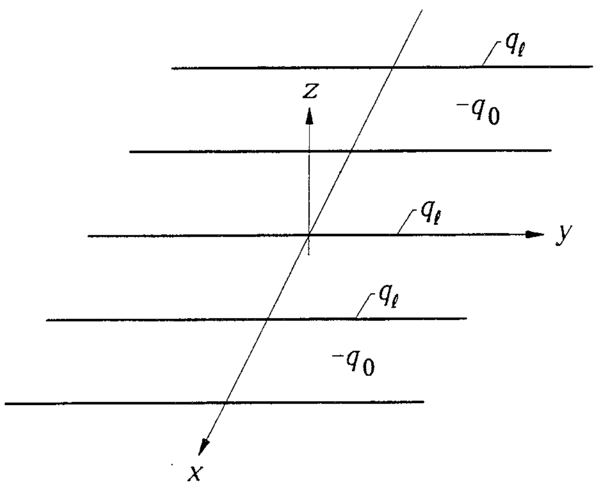

Figure 4: The line heat sources of strength q_l balanced by a plane heat sink of strength $-q_0$.

The second part is the contribution from a line of point heat sources of strength Q_0 along the central tunnel (y-axis) balanced by a line heat sink of strength $-q_l$ (See Figure 5). The third and last part is the contribution from a finite line heat source of strength q_c balanced by a point heat sink of strength $-Q_0$ (See Figure 6). Adding heat sources in Figures 4-6 give the heat sources in Figure 3. The different parts of T_{loc} will be presented in the following sections.

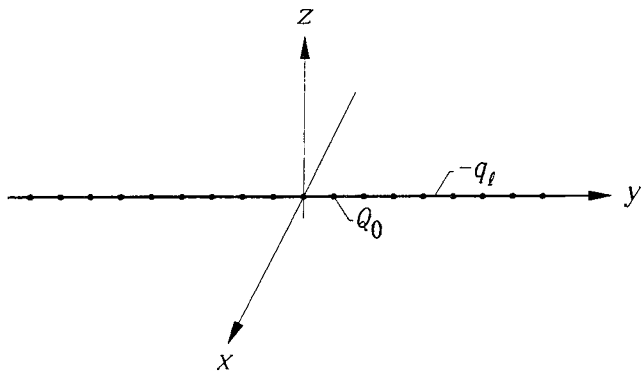

Figure 5: Point heat sources of strength Q_0 balanced by a line heat sink of strength $-q_l$ along the central tunnel.

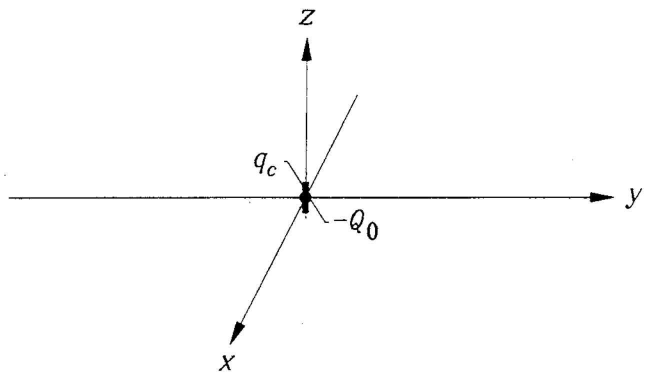

Figure 6: A finite line heat source of strength q_c along the central canister balanced by a point heat sink of strength $-Q_0$.

The local solution is valid for all interior canisters. In the case above the central canister was chosen as a representative of an interior canister. In other words, the local solution is applicable to any other canister that is not too close to the edges of the repository.

The local solution will be a quasi steady-state one, where the constant Q_0 in the steady-state solution will be replaced by the slowly varying $Q_0(t)$. See Section 9.

3.1 Line heat sources along tunnels

The temperature field caused by an infinite number of line heat sources balanced by a plane heat sink is given below. The line heat sources are spaced along the x-axis at D' intervals and they are parallel to the y-axis (See Figure 4). The strength of the line heat sources is $q_l(t) = Q_o(t)/D$ (W/m). We have:

$$T_{l.s.}(x, z) = \frac{Q_0}{2\pi\lambda D} T'_{l.s.}(x/D', z/D') \tag{9}$$

The dimensionless temperature $T'_{l.s.}$ is a function of dimensionless variables x/D' and z/D'. We have:

$$T'_{l.s.}(x', z') = -\frac{1}{2} \ln \left[1 - 2e^{-2\pi|z'|} \cdot \cos(2\pi x') + e^{-4\pi|z'|}\right] \tag{10}$$

The level curves of the dimensionless temperature $T'_{l.s.}$ are shown in Figure 7 for $-0.5 \le x' \le 0.5$ and $-1 \le z' \le 1$. The temperature is infinite at the line source at $x' = 0$ and $z' = 0$. The temperature tends to zero for large z'. The plane sink $-q_o$ along $z' = 0$ is seen as an edge in the level curves.

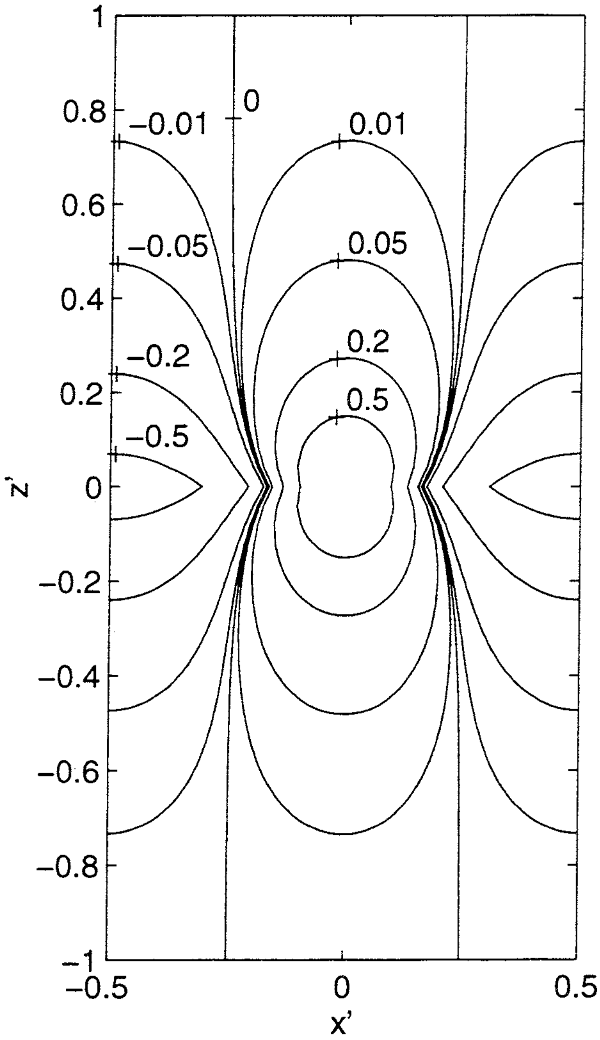

Figure 7: Level curves of the dimensionless temperature $T'_{l.s.}$.

3.2 Point heat sources along a tunnel

The temperature field caused by an infinite number of point heat sources Q_0 (W) along a line and a balancing line heat sink $-q_l$ (W/m) is given below. The point heat sources are spaced along the y-axis at D intervals (See Figure 5). We have:

$$T_{p.s.}(x, y, z) = \frac{Q_0}{2\pi\lambda D} T'_{p.s.}(y/D, \sqrt{x^2 + z^2}/D) \tag{11}$$

The dimensionless temperature $T'_{p.s.}$ is a function of dimensionless variables y/D and $\sqrt{x^2+z^2}/D$. We have:

$$T'_{p.s.}(y',\rho') = 2\sum_{n=1}^{\infty}\left[\cos\left(2\pi n y'\right) K_0\left(2\pi n \rho'\right)\right] \qquad \rho' = \sqrt{x^2+z^2}/D \tag{12}$$

The level curves of the dimensionless temperature $T'_{p.s.}$ are shown in Figure 8 for $-0.5 \le y' \le 0.5$ and $0 < \rho' \le 0.5$. The temperature is infinite (positive) at the point source at $y' = 0$ and $\rho' = 0$. The temperature tends to minus infinity at the y'-axis ($y' \neq 0$) due to the line heat sink $-q_l$.

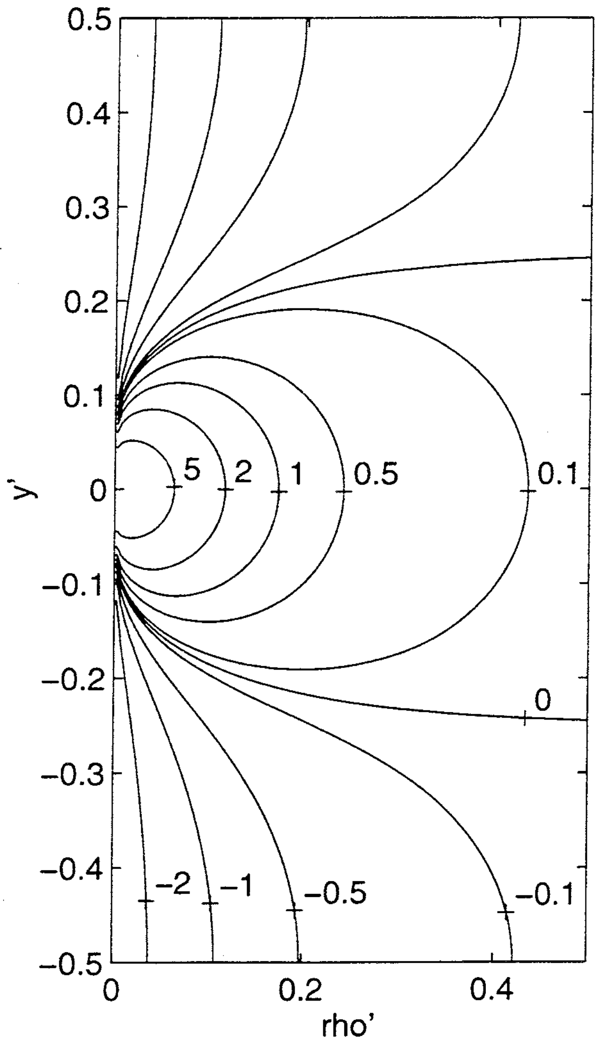

Figure 8: The level curves of the dimensionless temperature $T'_{p.s.}$.

3.3 Line heat source along a canister

The temperature field of a finite line heat source along a canister balanced by a point heat sink, Figure 6, is given by:

$$T_{l.c.}(x,y,z) = \frac{Q_0}{4\pi\lambda H_c} \cdot T'_{l.c.}\left(\sqrt{(2x/H_c)^2+(2y/H_c)^2}, 2z/H_c\right) \tag{13}$$

The dimensionless temperature $T'_{l.c.}$ is a function of dimensionless variables $\sqrt{(2x/H_c)^2 + (2y/H_c)^2}$ and $2z/H_c$. We have:

$$T'_{l.c.}(\rho'', z') = \ln\left(\frac{\sqrt{(\rho'')^2 + (1+z')^2} + 1 + z'}{\sqrt{(\rho'')^2 + (1-z')^2} - 1 + z'}\right) - \frac{2}{\sqrt{(\rho'')^2 + (z')^2}}$$

$$\rho'' = \sqrt{(2x/H_c)^2 + (2y/H_c)^2} \qquad (14)$$

The last term represents the balancing point heat sink.

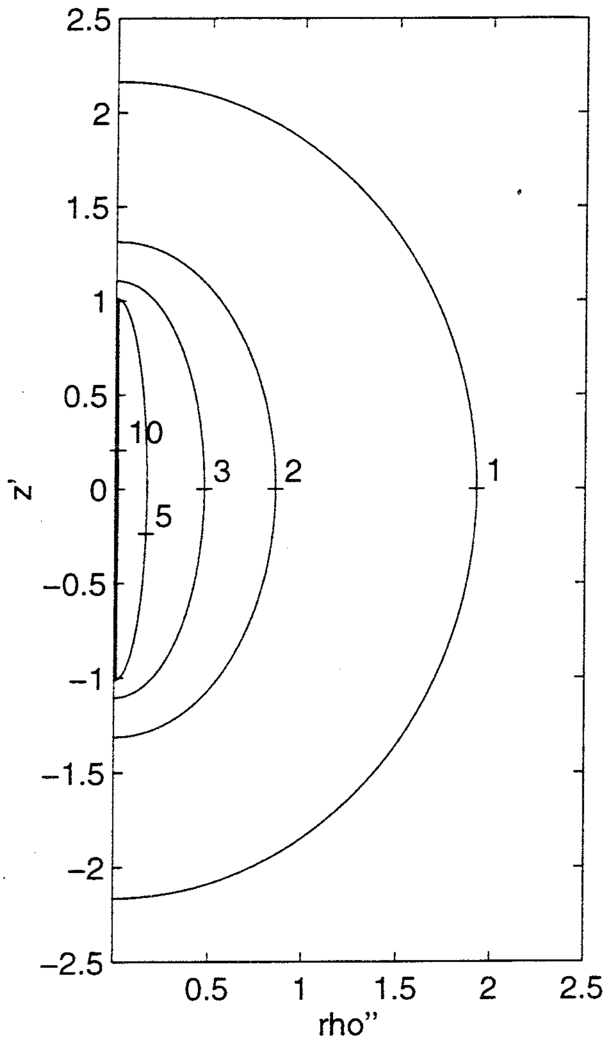

Figure 9: The level curves of the dimensionless temperature T'_{lcan}.

The temperature field T_{lcan} from the line heat source along the canister, $-H_c/2 \le z \le H_c/2$, with strength $Q_0(t)/H_c$ (W/m) is given by the first term of $T'_{l.c.}$ in Eq. (14). We have:

$$T_{lcan}(x, y, z) = \frac{Q_0}{4\pi\lambda H_c} \cdot T'_{lcan}(\rho'', z') \qquad (15)$$

The dimensionless temperature is given by:

$$T'_{lcan}(\rho'', z') = \ln\left(\frac{\sqrt{(\rho'')^2 + (1+z')^2} + 1 + z'}{\sqrt{(\rho'')^2 + (1-z')^2} - 1 + z'}\right) \qquad (16)$$

The level curves of the dimensionless temperature T'_{lcan} are shown in Figure 9 for $-2.5 \leq z' \leq 2.5$ and $0 < \rho'' \leq 2.5$. The temperature is infinite (positive) at the finite line heat source $\rho'' = 0$, $-1 \leq z \leq 1$.

3.4 Total local solution

The local temperature field induced by the heat sources in Figure 3 is given by:

$$T_{loc}(x,y,z;t) = \frac{Q_0(t)}{2\pi\lambda D} \cdot T'_{l.s.}\left(x/D', z/D'\right) + \frac{Q_0(t)}{2\pi\lambda D} \cdot T'_{p.s.}\left(y/D, \sqrt{x^2+z^2}/D\right)$$
$$+ \frac{Q_0(t)}{4\pi\lambda H_c} \cdot T'_{l.c.}\left(2\sqrt{x^2+y^2}/H_c, 2z/H_c\right) \tag{17}$$

4 Input data

The input data can be divided into three parts concerning the geometry of the heat-source, properties of the heat source and thermal properties of the rock. The following data are used in the reference case:

$$L = 500 \text{ m} \quad B = 500 \text{ m} \quad H = 500 \text{ m} \quad D = 6 \text{ m} \quad D' = 25 \text{ m}$$
$$H_c = 5 \quad R_c = 0.4 \text{ m}$$
$$q_1 = 5 \text{ W/m}^2 \quad q_2 = 5/3 \text{ W/m}^2 \quad t_1 = 46 \text{ y} \quad t_2 = 780 \text{ y}$$
$$C = \rho c = 2700 \cdot 800 \text{ J/(m}^3\text{K)} \quad \lambda = 3.5 \text{ W/(m} \cdot \text{K)} \tag{18}$$

The heat release from each canister is given by two exponentials:

$$Q_0(t) = Q_1 \cdot e^{-t/t_1} + Q_2 \cdot e^{-t/t_2} \qquad \text{(W)} \qquad Q_0(0) = 1000 \text{ W} \tag{19}$$

The heat release per unit area of the heat source is:

$$q_0(t) = q_1 \cdot e^{-t/t_1} + q_2 \cdot e^{-t/t_2} \qquad \text{(W/m}^2\text{)} \qquad q_i = Q_i/(DD')\ i = 1,2 \tag{20}$$

The total initial effect emitted from a canister is $Q_0(0)$ =1000 W. This effect is divided between the two decay components at a ratio 3:1 (750 W/250 W). The initial amplitude of the heat emission rate with the decay time $t_1 = 46$ years is Q_1 =750 W (3/4 of 1000 W) for each canister. The area around a canister is $DD' = 6 \cdot 25$ m^2. The effect per unit area q_1 is then $750/150 = 5$ W/m^2. The second effect Q_2 with the longer decay time t_2 =780 years has initially one fourth of the total initial effect $Q_0(0)$ or a third of Q_1. In this case $Q_2 = 250$ W.

The expression (19) for the heat release is valid for the first 1000 years. The effect release is erroneous for times longer than 1000 years. The error increases with time. An expression that is valid for longer times has been derived in (Hökmark H, 1996). This expression for the heat release will be used in Section 8 where the global temperature field for times longer than 1000 years is discussed.

All results presented in this study concern the above reference case.

5 Numerical model

The solution for the total (global and local) temperature field has been implemented on PC for rapid computer solution. This is described in greater detail in Appendix 1. Briefly, the model is implemented in MATLAB version 4.2c.1 and run on a Intel Pentium 90 MHz PC.

The calculation of the total temperature at a point takes roughly 3 seconds. This execution time depends strongly on the number of modified bessel functions used in the sum of Eq. (12). The time integral in the global solution is evaluated numerically.

All the figures showing temperature fields have been generated by MATLAB. The resolution and execution times for temperature fields illustrated in the figures are given in Appendix 1.

6 The total solution

The total solution is given by the sum of the global solution, the local solution and the undisturbed temperature $T_0(z)$. We have:

$$T_{tot}(x,y,z,t) = T_{gl}(x,y,z,t) + T_{loc}(x,y,z,t) + T_0(z) \tag{21}$$

The undisturbed temperature of the ground $T_0(z)$ is given in (Israelsson J, 1995). The temperature at the ground surface is set to 7°C and the constant downward gradient is set to 0.016°C/m, which corresponds to a temperature of 15°C at the repository level (H=500 m). Near the repository plane the undisturbed temperature $T_0(z)$ can be approximated by $T_{rep,0} = 15$°C. We have:

$$T_{tot}(x,y,z,t) = T_{gl}(x,y,z,t) + T_{loc}(x,y,z,t) + T_{rep,0} \tag{22}$$

The global solution is approximately constant in the repository plane. In this case we get the total solution by adding a constant temperature to T_{loc}. The global temperature is 33.9° C for $t = 50$ years and 34.3° C for $t = 500$ years. In the vertical cross-section through the repository, planes $y = 0$ and $x = 0$, the temperature changes by a few degrees in the z-direction from the centre of the plane $z = 0$ to $z = \pm 2H_c$. In the case $t = 50$ and 500 years the temperature difference is 4.6 °C and 1.3 °C, respectively (KBS-3 data).

7 Total temperature field

The local solution is periodic in the x- and y-directions except near the edges of the repository (with the period D' and D, respectively). The global solution is constant in planes parallel and close to the repository plane. Furthermore, the total local temperature field is small for $z \geq 2H_c$ (In the KBS-3 case $T_{loc}(0,0,2H_c,50) = 0.3$°C). This means that we only need to look at the total solution in a parallelepiped surrounding the central canister to get the essential behaviour of the temperature field. See Figure 10. The parallelepiped surrounding the central canister is defined by:

$$\begin{cases} -D'/2 \leq x \leq D'/2 \\ -D/2 \leq y \leq D/2 \\ -2H_c \leq z \leq 2H_c \end{cases} \tag{23}$$

The temperature field of the total solution is studied for $t = 50$ years. The largest canister temperature occurs after 43 years, and the largest global temperature occurs after 82 years (according to (Claesson J, Probert T, Jan. 1996)). The total solution will be shown in six cross-sections of the parallelepiped (two horizontal and four vertical). Three of the cross-sections, $x = 0$, $y = 0$ and $z = 0$, intersect at the centre of the parallelepiped (Also the centre of the central canister). The remaining horizontal cross-section cuts the parallelepiped at $z = H_c$. The last two cross-sections are two of the vertical faces of the parallelepiped, $x = D'/2$ and $y = D/2$. The solution in the parallelepiped is symmetrical in the x-, y- and z-directions with respect to the centre (0, 0, 0) which reduces the number of calculations by 75%.

In all the temperature fields the 57°C level curve is shown. This temperature is the canister temperature after 50 years as determined in (Claesson J, Probert T, Jan. 1996).

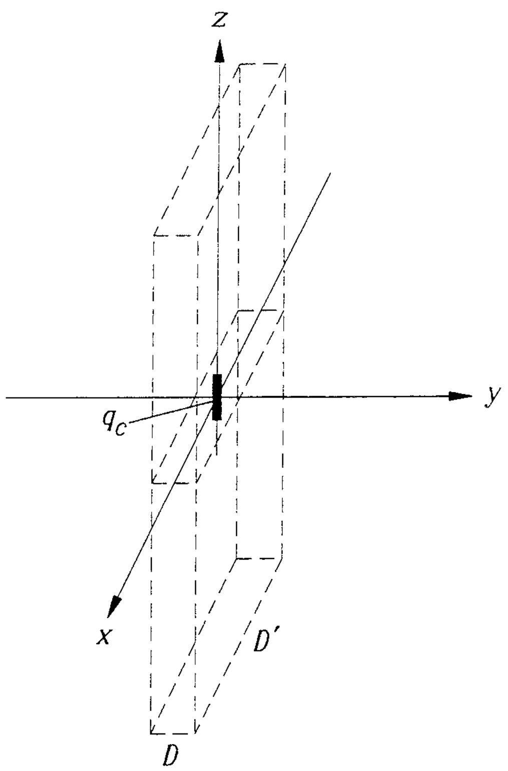

Figure 10: The parallelepiped surrounding the central canister. The total local solution is illustrated in planes that are vertical and horizontal cross-sections of this volume.

In Figure 11 the total temperature field is shown in the horizontal plane $z = 0$ through the centre of the parallelepiped. The circular 57-degree isotherm corresponds roughly to the radius (0.4 m) of the canister. The 48-degree isotherm is nearly straight.

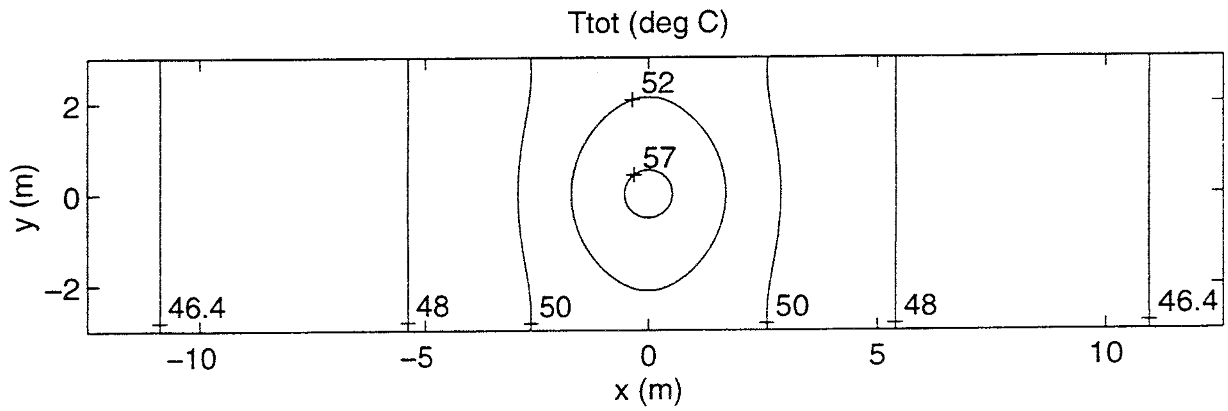

Figure 11: The total temperature field T_{tot} in the plane: $-D'/2 \leq x \leq D'/2$, $-D/2 \leq y \leq D/2$, $z = 0$ ($t = 50$ years).

In Figure 12 the total temperature field is shown in the vertical plane $y = 0$ through the centre of the parallelepiped. The elliptical 57-degree isotherm corresponds roughly to the cylindrical shape of the canister (length= 5 m, radius= 0.4 m).

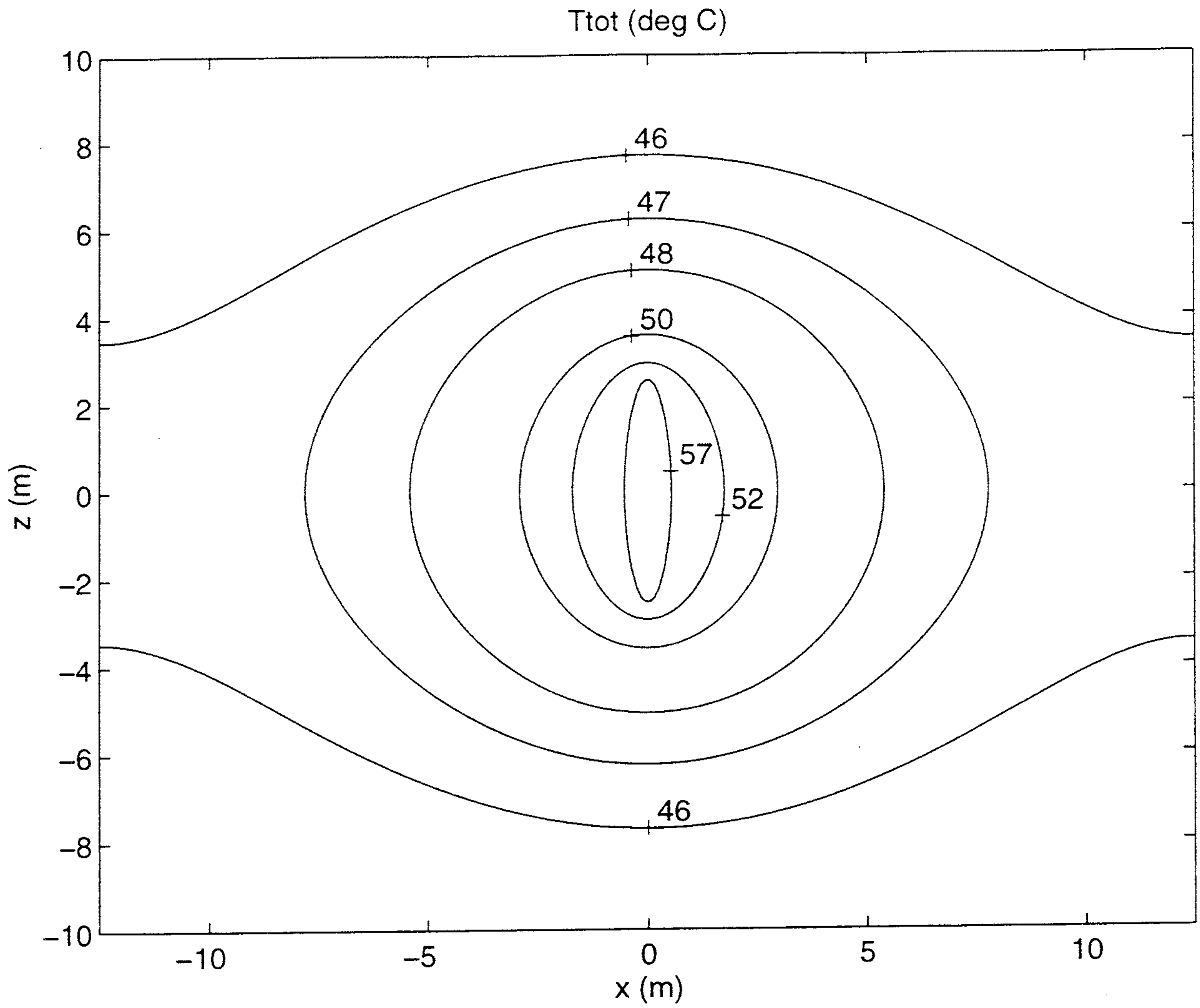

Figure 12: The total temperature field T_{tot} in the plane: $-D'/2 \leq x \leq D'/2$, $y = 0$, $-2H_c \leq z \leq 2H_c$ ($t = 50$ years).

In Figure 13 the total temperature field is shown in the vertical plane $x = 0$ through the centre of the parallelepiped. The elliptical 57-degree isotherm corresponds roughly to the cylindrical shape of the canister (length= 5 m, radius= 0.4 m). isotherm does not. The 46-degree isotherm is nearly straight.

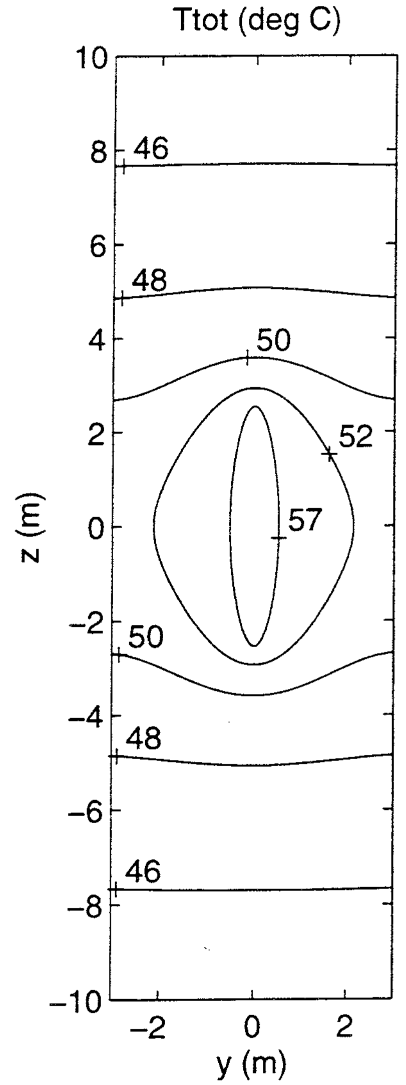

Figure 13: The total temperature field T_{tot} in the plane: $x = 0$, $-D/2 \leq y \leq D/2$, $-2H_c \leq z \leq 2H_c$ ($t = 50$ years).

In Figure 14 the total temperature field is shown in the vertical plane $y = D/2$, which is a face of the parallelepiped. This plane is 3 metres from the centre of the canister.

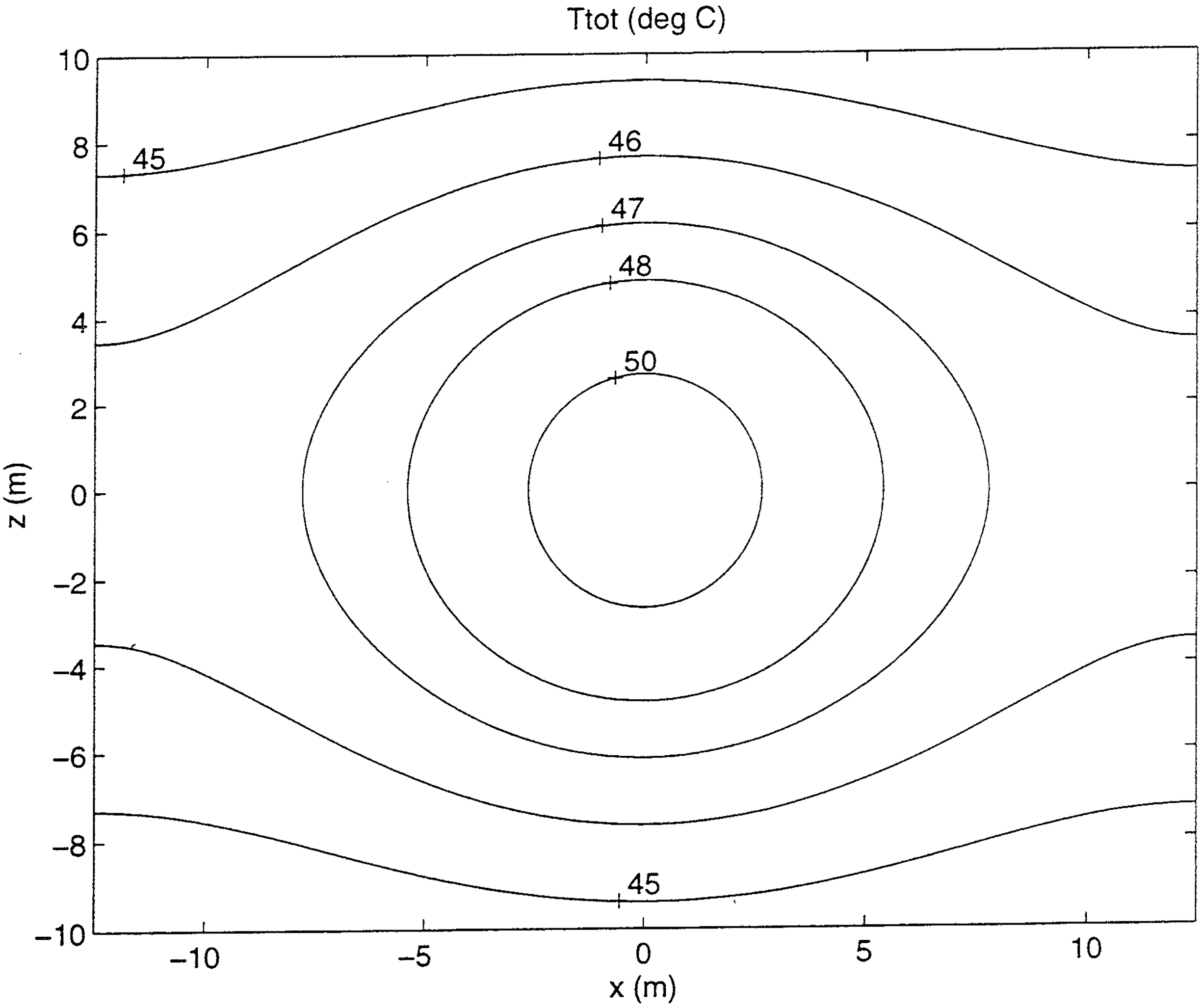

Figure 14: The total temperature field T_{tot} in the plane: $-D'/2 \leq x \leq D'/2$, $y = D/2$, $-2H_c \leq z \leq 2H_c$ ($t = 50$ years).

In Figure 15 the total temperature field is shown in the vertical plane $x = D'/2$, which is a face of the parallelepiped. This plane is 12.5 metres from the centre of the canister. The 45- and 46-degree isotherms are straight.

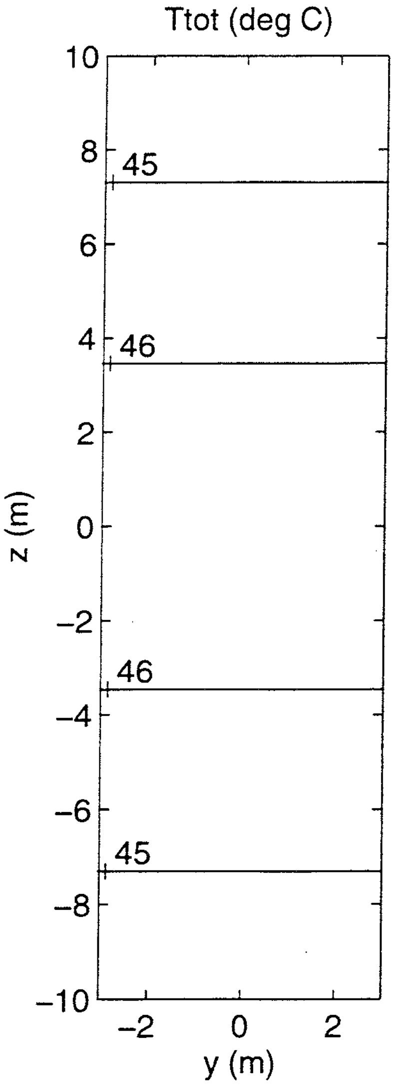

Figure 15: The total temperature field T_{tot} in the plane: $x = D'/2$, $-D/2 \leq y \leq D/2$, $-2H_c \leq z \leq 2H_c$ ($t = 50$ years).

In Figure 16 the total temperature field is shown in the horizontal plane $z = H_c$. This horizontal cross-section is 2.5 metres above the canister. The 48-degree isotherm is elliptical in shape. The 47-degree isotherm is nearly straight.

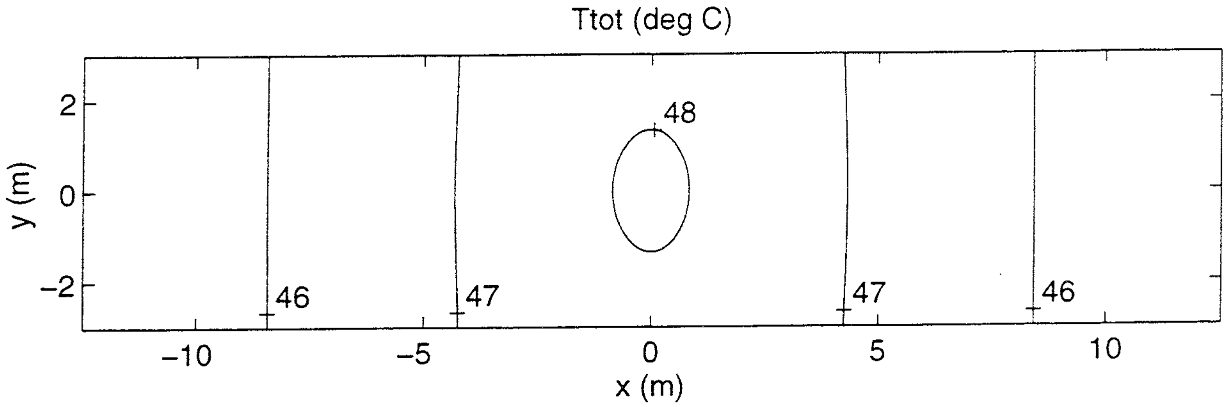

Figure 16: The total temperature field T_{tot} in the plane: $-D'/2 \leq x \leq D'/2$, $-D/2 \leq y \leq D/2$, $z = H_c$ ($t = 50$ years).

8 Global temperature field for times longer than 1000 years

The expression (19) in Section 4 for the heat release is valid for the first 1000 years. After 1000 years the effect release is under estimated. Accuracy is increased by using three exponentials instead of two in the expression for the heat release. The new expression for the heat release, which is valid for 10 000 years, is obtained by least square approximation to fit the effect curve in (SKB 91, 1992) to three exponentials with the decay times:

$$t_1 = 50 \qquad t_2 = 500 \qquad t_3 = 5000 \qquad \text{(years)} \tag{24}$$

The heat release from each canister is then given by three exponentials:

$$Q_0(t) = Q_1 \cdot e^{-t/t_1} + Q_2 \cdot e^{-t/t_2} + Q_3 \cdot e^{-t/t_3} \qquad \text{(W)} \qquad Q_0(0) = 1000 \text{ W} \tag{25}$$

The total initial effect emitted from a canister is $Q_0(0)$ =1000 W. This effect is divided between the three decay components so that:

$$Q_1 = 770 \qquad Q_2 = 163 \qquad Q_3 = 67 \qquad \text{(W)} \tag{26}$$

The expression for the heat release (25) is derived in (Hökmark H, 1996).

In Figure 17 the temporal development of the temperature field is shown at the centre of the repository for $0 \leq t \leq 10000$ years (left), and for $0 \leq t \leq 500$ years (right). It should be noted that the temperature is the excess temperature above the undisturbed temperature. The temperature increases rapidly during the first ten years because of the heat release. Then the temperature increase gradually becomes smaller until a maximum is reached, and the temperature starts to decrease because of the exponential nature of the heat source. The maximum temperature of approximately 35°C occurs after 80 odd years. There is no minimum or second maximum, just a slightly slanted stretch from 200 to 500 years. The exponential with the longest decay time takes over after roughly 2000 years. Compare Figure 17 with Figure 5 of (Probert T, Claesson J, Apr. 1996).

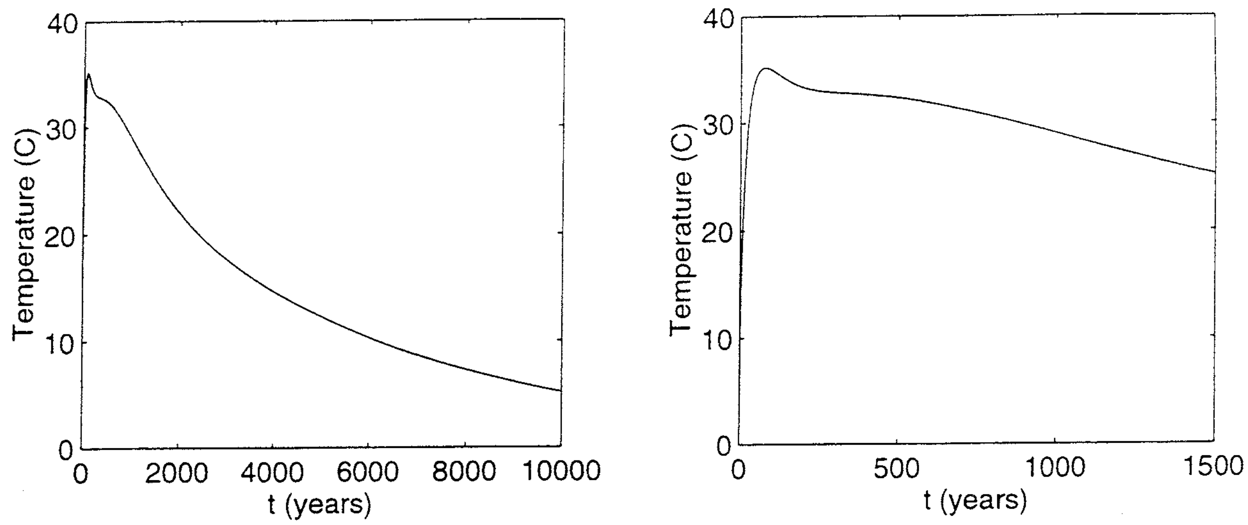

Figure 17: The temperature at the centre of the repository for $0 \leq t \leq 10\,000$ (left) and for $0 \leq t \leq 1500$ (right).

The temperature field along the z-axis is shown in Figure 18 for three times, $t = 1000$, 5000 and 10 000 years. The maximum temperature along the z-axis is reached at the repository centre $z = 0$. The maximum temperature is 28, 12 and 5°C after 1000, 5000 and 10 000 years, respectively.

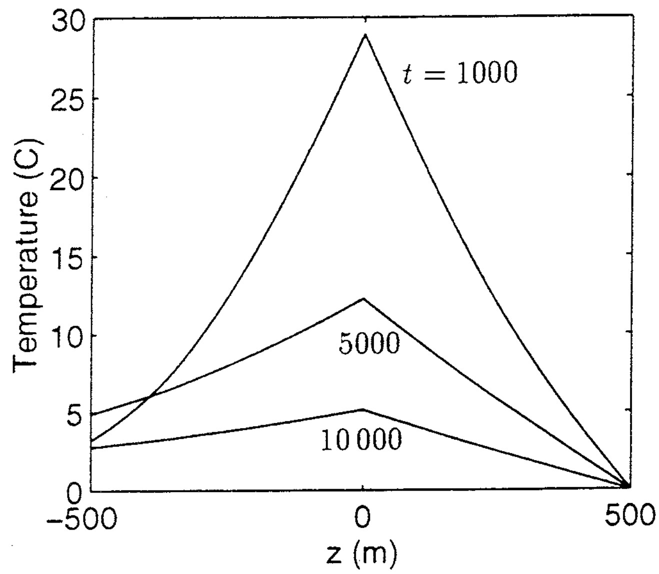

Figure 18: The temperature along the z-axis, from the ground surface at $z = 500$ to $z = -500$ via the centre, for three times t =1000, 5000 and 10 000 years.

The temperature along the x-axis is shown in Figure 19 for three times, $t = 1000$, 5000 and 10 000 years. The maximum temperature along the x-axis is reached at the repository centre $x = 0$. The maximum temperature is 28, 12 and 5°C after 1000, 5000 and 10 000 years, respectively.

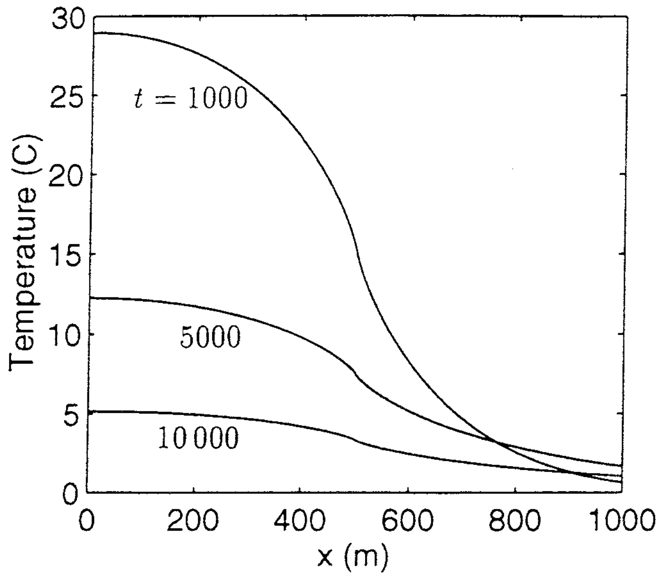

Figure 19: The temperature along the x-axis, from the centre to x = 1000, for three times t =1000, 5000 and 10 000 years.

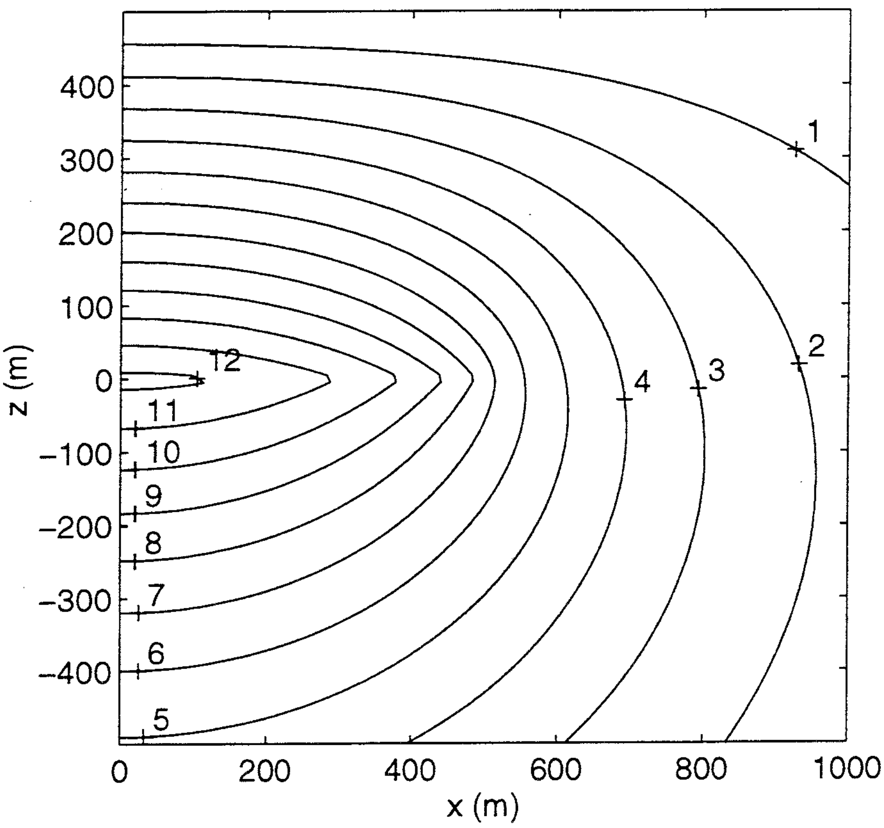

Figure 20: The temperature field in the vertical plane $y = 0$ for $t = 5000$ years.

The temperature field in the vertical plane $y = 0$ is shown in Figures 20 and 21 for t =5000 and 10 000 years, respectively. The level curves of the temperature field are shown for the integer values from 1 to 12°C in Figure 20, and for the integer values from 1 to 5°C in Figure 21. The level curves in both figures encircle the repository at $0 \leq x \leq 500$, $z = 0$. The excess temperature 100 metres below the ground surface is 2°C and 1°C after 5000 and 10 000 years, respectively. The isotherms are more dispersed for t = 10 000 years.

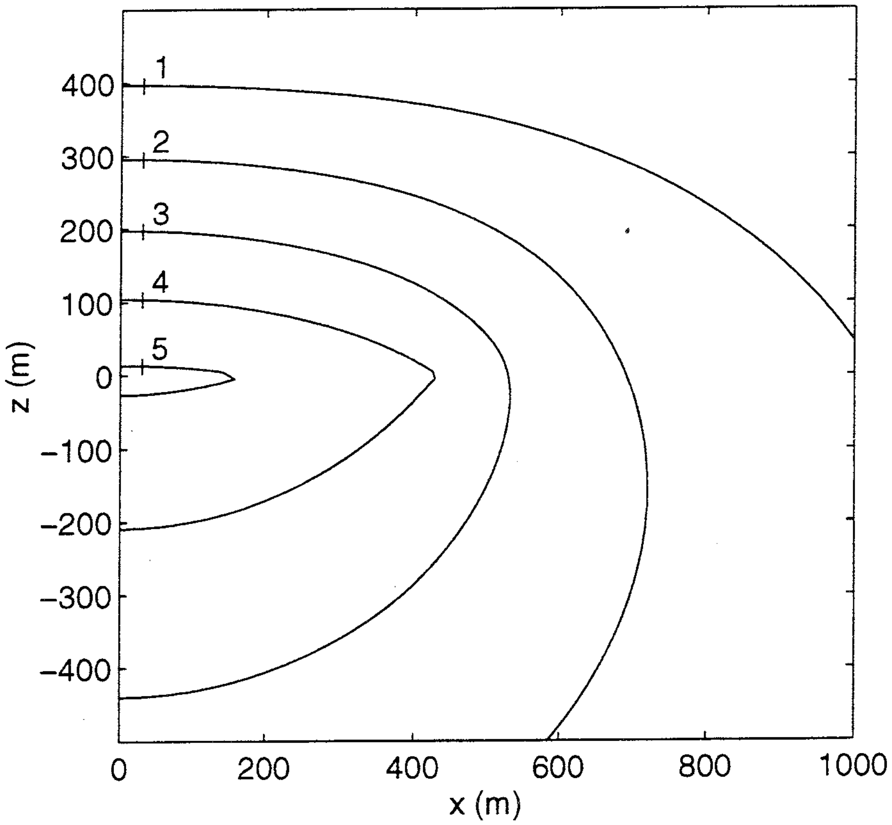

Figure 21: The temperature field in the vertical plane $y = 0$ for t =10 000 years.

The temperature field in the horizontal plane $z = 0$ is shown in Figures 22 and 23 for t =5000 and 10 000 years, respectively. The level curves of the temperature field are shown for the integer values from 1 to 12°C in Figure 22, and for the integer values from 1 to 5°C in Figure 23. The level curves encircle the repository at $0 \leq x, y \leq 500$. The isotherms are more dispersed for t = 10 000 years.

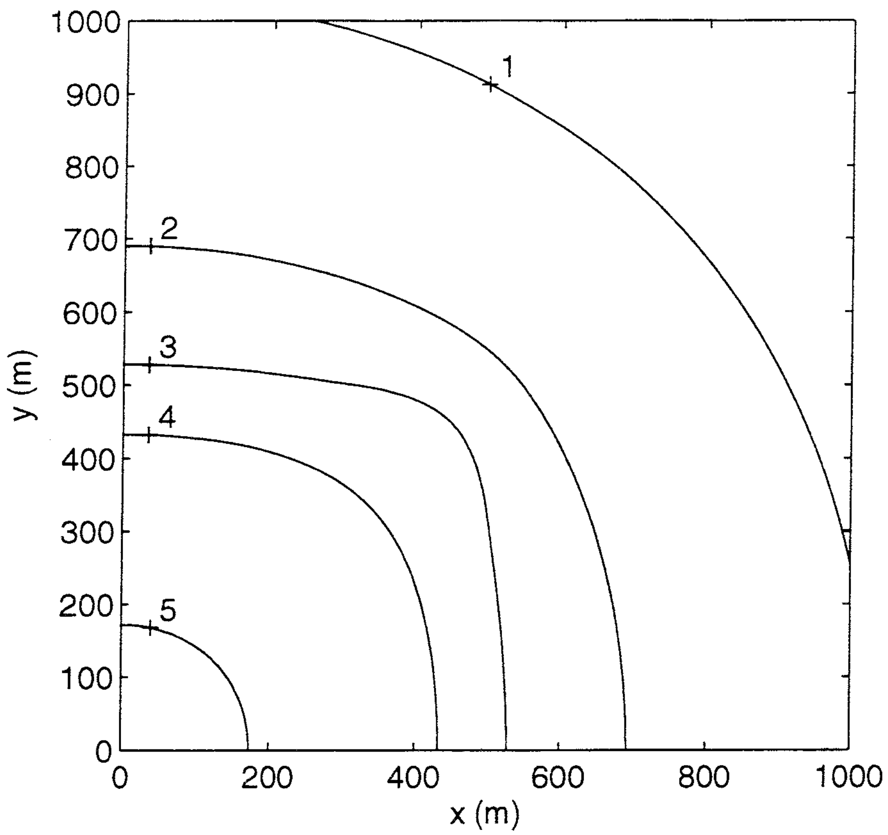

Figure 22: The temperature field in the horizontal plane $z = 0$ for $t = 5000$ years.

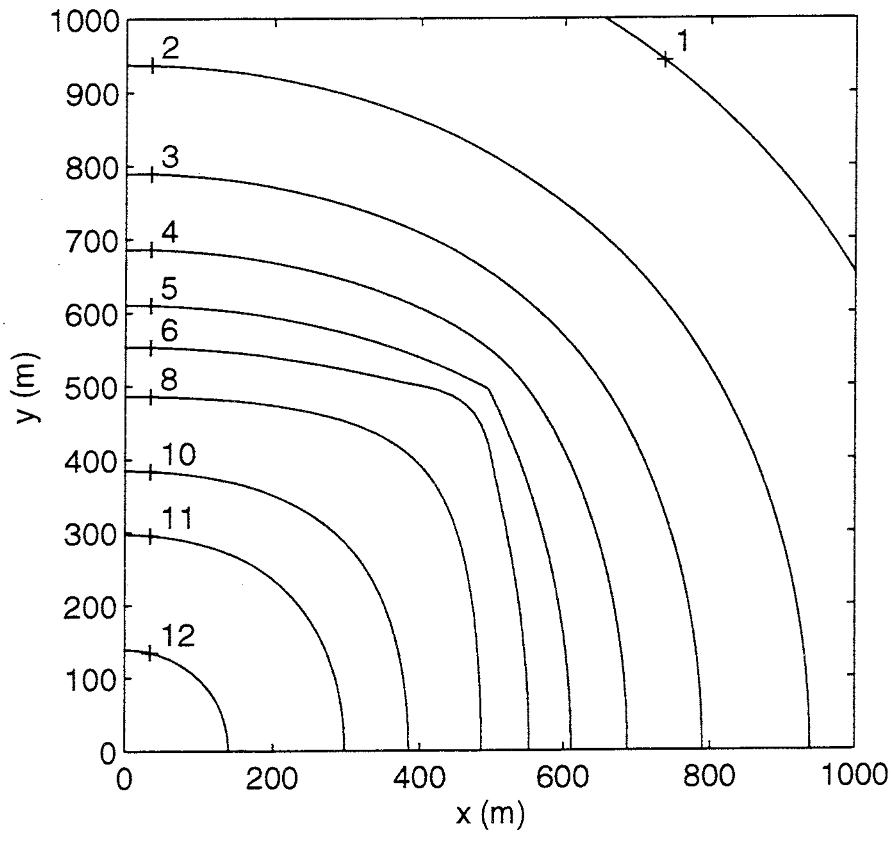

Figure 23: The temperature field in the horizontal plane $z = 0$ for $t = 10\,000$ years.

If the global temperature field is to be studied for times longer than 10 000 years then a new expression for the heat release must be derived. This expression will consist of four or more exponentials with even longer decay times.

9 Quasi steady-state local solution

The variation of $Q_0(t)$ with time is quite slow in the KBS-3 case, since the lowest time scale is $t_1 = 46$ years. The time-scale to attain steady-state conditions for constant $Q_0 = q_0 \cdot DD'$ in the balanced case turns out to be a few years only. This has been verified by numerical calculations performed by Thomas Blomberg, Dept. of Building Physics, Lund Institute of Technology. The solution will be a quasi steady-state one, where the constant Q_0 in the steady-state solution will be replaced by the slowly varying $Q_0(t)$.

References

Claesson J, Hellström G, 1995. Thermoelastic Stress Due to an Instantaneous Finite Line Heat Source in an Infinite Medium. Dept. of Mathematical Physics, Lund University, Sweden. SKB Technical Report TR 96-11.

Claesson J, Probert T, Jan. 1996. Temperature Field due to Time-Dependent Heat Sources in a Large Rectangular Grid. I. Derivation of an analytical solution. Dept. of Mathematical Physics, Lund University, Sweden. SKB Technical Report TR 96-12.

Claesson J, Probert T, May 1996. Thermoelastic Stress due to a Rectangular Heat Source in a Semi-infinite Medium. I. Derivation of an analytical solution. Dept. of Mathematical Physics, Lund University, Sweden. SKB Technical Report TR 96-13.

Hökmark H, 1996. Canister Positioning - Stage 1 Thermomechanical Nearfield Rock Analysis. SKB Report AR D-96-014.

Israelsson J, June 1995. Global Thermo-Mechanical Effects from a KBS-3 Type Repository, Phase 1; Elastic Analyses. Itasca Geomekanik AB, Borlänge, Sweden.

Probert T, Claesson J, April 1997. Thermoelastic Stress due to a Rectangular Heat Source in a Semi-infinite Medium. II. Application for the KBS-3 repository.. Dept. of Mathematical Physics, Lund University, Sweden. (To be published as a SKB Technical Report.)

Appendix 1. Manual for the computer code

Introduction

This short manual describes how to use the computer model that calculates the temperature fields derived in Claesson, Probert (Jan. 1996) and applied in this paper. The numerical model is implemented in MATLAB version 4.2c.1 in the Windows 3.11 milieu run on DOS 6.22. The numerical solution has the same structure as Eqs (3), (4), (17) and (21).

The m-files

Nine m-files are used. These m-files are:

- **ttot.m** (T_{tot})
- **tgl.m** (T_{gl})
- **tgli.m** ($T_{gl,i}$)
- **tloc.m** (T_{loc})
- **tls.m** ($T_{l.s.}$)
- **tps.m** ($T_{p.s.}$)
- **tlc.m** ($T_{l.c.}$)
- **q0t0.m** ($Q_0(t)$)
- **constst.m**

The first seven are function files and the last is a script file. The corresponding temperature calculated or value initiated by the function m-files is shown in brackets after the m-file name. The function **ttot** calls the functions **tgl** and **tloc**. The function **tgl** calls the function **tgli**, and the function **tloc** calls the functions **tls**, **tps** and **tlc**. All function files, directly or indirectly, call **constst**. The function m-file **q0t0** is only called by the functions **tls**, **tps** and **tlc**.

The input is initiated by the script m-file **constst**. The input data consists of five parts:

- Geometry of the repository with tunnel spacings and canister dimensions (L, B, H, D, D', H_c, R_c)
- Mechanical properties of the rock mass (ρ)
- Thermal properties of the rock mass (c, λ, a)
- Heat source data ($Q_0(0)$, $q_i(0)$, t_i)
- Undisturbed temperature ($T_{rep,0}$)

Any item of input data may be altered. If the number of exponentials is changed then the number of decay times t_i and initial heat releases q_i must be changed accordingly in the m-files **tgl** and **constst**, and in the global variable declarations.

The calculation of the local temperature at a point takes roughly 1-3 seconds. This execution time depends strongly on the number of modified bessel functions used in the sum of Eq. (12). The number of terms depends on the rate of convergence and the accuracy that is needed. The rate of convergence varies from point to point. If 50 terms are used the execution time is less than 1 second. If, however, 400 terms are used the execution time is over 3 seconds.

The global temperature takes slightly less than 1 second to calculate. This time depends on the size of the arguments in the Error function calls and the number of Error function calls. An Error function call takes between 5 and 8 milliseconds. The number of Error function calls needed depends on the integration procedure. The time integral in the global solution is evaluated numerically using the Trapezoidal rule with $n = 300$. This value of n gives the integral value with an error less than 1% of the integral value for $n = 10\,000$. If $n = 300$ the execution time is roughly half a second. If $n = 1000$ the execution time is roughly a second.

All the figures showing temperature fields have been generated by MATLAB. The resolution and execution times for the illustrated temperature fields in the figures are the following. The figures in Section 3 have a resolution of 100×200 points with the exception of Figure 7 which has 200×200 points. Figures 7 and 9 were drawn directly and Figure 8 took 8 hours. The Figures in Section 7 have a resolution of 200×200 points and they took 8 hours each. Note that only 100×100 points were used in all the calculations because of symmetry.

List of SKB reports

Annual Reports

1977-78
TR 121
KBS Technical Reports 1 – 120
Summaries
Stockholm, May 1979

1979
TR 79-28
The KBS Annual Report 1979
KBS Technical Reports 79-01 – 79-27
Summaries
Stockholm, March 1980

1980
TR 80-26
The KBS Annual Report 1980
KBS Technical Reports 80-01 – 80-25
Summaries
Stockholm, March 1981

1981
TR 81-17
The KBS Annual Report 1981
KBS Technical Reports 81-01 – 81-16
Summaries
Stockholm, April 1982

1982
TR 82-28
The KBS Annual Report 1982
KBS Technical Reports 82-01 – 82-27
Summaries
Stockholm, July 1983

1983
TR 83-77
The KBS Annual Report 1983
KBS Technical Reports 83-01 – 83-76
Summaries
Stockholm, June 1984

1984
TR 85-01
Annual Research and Development Report 1984
Including Summaries of Technical Reports Issued during 1984. (Technical Reports 84-01 – 84-19)
Stockholm, June 1985

1985
TR 85-20
Annual Research and Development Report 1985
Including Summaries of Technical Reports Issued during 1985. (Technical Reports 85-01 – 85-19)
Stockholm, May 1986

1986
TR 86-31
SKB Annual Report 1986
Including Summaries of Technical Reports Issued during 1986
Stockholm, May 1987

1987
TR 87-33
SKB Annual Report 1987
Including Summaries of Technical Reports Issued during 1987
Stockholm, May 1988

1988
TR 88-32
SKB Annual Report 1988
Including Summaries of Technical Reports Issued during 1988
Stockholm, May 1989

1989
TR 89-40
SKB Annual Report 1989
Including Summaries of Technical Reports Issued during 1989
Stockholm, May 1990

1990
TR 90-46
SKB Annual Report 1990
Including Summaries of Technical Reports Issued during 1990
Stockholm, May 1991

1991
TR 91-64
SKB Annual Report 1991
Including Summaries of Technical Reports Issued during 1991
Stockholm, April 1992

1992
TR 92-46
SKB Annual Report 1992
Including Summaries of Technical Reports Issued during 1992
Stockholm, May 1993

1993
TR 93-34
SKB Annual Report 1993
Including Summaries of Technical Reports Issued during 1993
Stockholm, May 1994

1994
TR 94-33
SKB Annual Report 1994
Including Summaries of Technical Reports Issued during 1994
Stockholm, May 1995

1995
TR 95-37
SKB Annual Report 1995
Including Summaries of Technical Reports Issued during 1995
Stockholm, May 1996

1996
TR 96-25
SKB Annual Report 1996
Including Summaries of Technical Reports Issued during 1996
Stockholm, May 1997

List of SKB Technical Reports 1997

TR 97-01
Retention mechanisms and the flow wetted surface – implications for safety analysis
Mark Elert
Kemakta Konsult AB
February 1997

TR 97-02
Äspö HRL – Geoscientific evaluation 1997/1. Overview of site characterization 1986–1995
Roy Stanfors[1], Mikael Erlström[2], Ingemar Markström[3]
[1] RS Consulting, Lund
[2] SGU, Lund
[3] Sydkraft Konsult, Malmö
March 1997

TR 97-03
Äspö HRL – Geoscientific evaluation 1997/2. Results from pre-investigations and detailed site characterization. Summary report
Ingvar Rhén (ed.)[1], Göran Bäckblom (ed.)[2], Gunnar Gustafson[3], Roy Stanfors[4], Peter Wikberg[2]
[1] VBB Viak, Göteborg
[2] SKB, Stockholm
[3] VBB Viak/CTH, Göteborg
[4] RS Consulting, Lund
May 1997

TR 97-04
Äspö HRL – Geoscientific evaluation 1997/3. Results from pre-investigations and detailed site characterization. Comparison of predictions and observations. Geology and mechanical stability
Roy Stanfors[1], Pär Olsson[2], Håkan Stille[3]
[1] RS Consulting, Lund
[2] Skanska, Stockholm
[3] KTH, Stockholm
May 1997

TR 97-05
Äspö HRL – Geoscientific evaluation 1997/4. Results from pre-investigations and detailed site characterization. Comparison of predictions and observations. Hydrogeology, groundwater chemistry and transport of solutes
Ingvar Rhén[1], Gunnar Gustafson[2], Peter Wikberg[3]
[1] VBB Viak, Göteborg
[2] VBB Viak/CTH, Göteborg
[3] SKB, Stockholm
June 1997

TR 97-06
Äspö HRL – Geoscientific evaluation 1997/5. Models based on site characterization 1986–1995
Ingvar Rhén (ed.)[1], Gunnar Gustafson[2], Roy Stanfors[3], Peter Wikberg[4]
[1] VBB Viak, Göteborg
[2] VBB Viak/CTH, Göteborg
[3] RS Consulting, Lund
[4] SKB, Stockholm
October 1997

TR 97-07
A methodology to estimate earthquake effects on fractures intersecting canister holes
Paul La Pointe, Peter Wallmann, Andrew Thomas, Sven Follin
Golder Associates Inc.
March 1997

TR 97-08
Äspö Hard Rock Laboratory Annual Report 1996
SKB
April 1997

TR 97-09
A regional analysis of groundwater flow and salinity distribution in the Äspö area
Urban Svensson
Computer-aided Fluid Engineering AB
May 1997

TR 97-10
On the flow of groundwater in closed tunnels. Generic hydrogeological modelling of nuclear waste repository, SFL 3–5
Johan G Holmén
Uppsala University/Golder Associates AB
June 1997

TR 97-11
Analysis of radioactive corrosion test specimens by means of ICP-MS. Comparison with earlier methods
R S Forsyth
Forsyth Consulting
July 1997

TR 97-12
Diffusion and sorption properties of radionuclides in compacted bentonite
Ji-Wei Yu, Ivars Neretnieks
Dept. of Chemical Engineering and Technology, Chemical Engineering, Royal Institute of Technology, Stockholm, Sweden
July 1997

TR 97-13
Spent nuclear fuel – how dangerous is it? A report from the project "Description of risk"
Allan Hedin
Swedish Nuclear Fuel and Waste Management Co,
Stockholm, Sweden
March 1997

TR 97-14
Water exchange estimates derived from forcing for the hydraulically coupled basins surrounding Äspö island and adjacent coastal water
Anders Engqvist
A & I Engqvist Konsult HB, Vaxholm, Sweden
August 1997

TR 97-15
Dissolution studies of synthetic soddyite and uranophane
Ignasi Casas[1], Isabel Pérez[1], Elena Torrero[1], Jordi Bruno[2], Esther Cera[2], Lara Duro[2]
[1] Dept. of Chemical Engineering, UPC
[2] QuantiSci SL
September 1997

TR 97-16
Groundwater flow through a natural fracture. Flow experiments and numerical modelling
Erik Larsson
Dept. of Geology, Chalmers University of Technology, Göteborg, Sweden
September 1997

TR 97-17
A site scale analysis of groundwater flow and salinity distribution in the Äspö area
Urban Svensson
Computer-aided Fluid Engineering AB
October 1997

TR 97-18
Release of segregated nuclides from spent fuel
L H Johnson, J C Tait
AECL, Whiteshell Laboratories, Pinawa, Manitoba, Canada
October 1997

TR 97-19
Assessment of a spent fuel disposal canister. Assessment studies for a copper canister with cast steel inner component
Alex E Bond, Andrew R Hoch, Gareth D Jones, Aleks J Tomczyk, Richard M Wiggin, William J Worraker
AEA Technology, Harwell, UK
May 1997

TR 97-20
Diffusion data in granite Recommended values
Yvonne Ohlsson, Ivars Neretnieks
Department of Chemical Engineering and Technology, Chemical Engineering, Royal Institute of Technology, Stockholm, Sweden
October 1997

TR 97-21
Investigation of the large scale regional hydrogeological situation at Ceberg
Anders Boghammar[1], Bertil Grundfelt[1], Lee Hartley[2]
[1] Kemakta Konsult AB, Sweden
[2] AEA Technology, UK
November 1997

TR 97-22
Investigations of subterranean microorganisms and their importance for performance assessment of radioactive waste disposal. Results and conclusions achieved during the period 1995 to 1997
Karsten Pedersen
Göteborg University, Institute of Cell and Molecular Biology, Dept. of General and Marine Microbiology, Göteborg, Sweden
November 1997

TR 97-23
Summary of hydrogeologic conditions at Aberg, Beberg and Ceberg
Douglas Walker[1], Ingvar Rhén[2], Ioana Gurban[1]
[1] INTERA KB
[2] VBB Viak
October 1997

TR 97-24
Characterization of the excavation disturbance caused by boring of the experimental full scale deposition holes in the Research Tunnel at Olkiluoto
Jorma Autio
Saanio & Riekkola Oy, Helsinki, Finland
September 1997

TR 97-25
The SKB Spent Fuel Corrosion Programme.
An evaluation of results from the experimental programme performed in the Studsvik Hot Cell Laboratory
Roy Forsyth
Forsyth Consulting
December 1997

TR 97-26
Thermoelastic stress due to a rectangular heat source in a semi-infinite medium. Application for the KBS-3 repository
Thomas Probert, Johan Claesson
Depts. of Mathematical Physics and Building Physics, Lund University, Sweden
April 1997

ISSN 0284-3757
CM Gruppen AB, Bromma, 1998